ResearchGate

See discussions, stats, and author profiles for this publication at: https://www.researchgate.net/publication/258468670

Tracking Lunar Dust – Analysis of Apollo Footage

Article · December 2011

CITATIONS
0

READS
1,090

2 authors, including:



Mihaly Horanyi
University of Colorado
621 PUBLICATIONS **7,462** CITATIONS

SEE PROFILE

Some of the authors of this publication are also working on these related projects:

Project Developing new dust trajectory sensor with single channel amplifier View project

Project Lunar magnetic anomalies View project

All content following this page was uploaded by Mihaly Horanyi on 28 December 2014.

The user has requested enhancement of the downloaded file.

Ballistic motion of dust particles in the Lunar Roving Vehicle dust trails

Hsiang-Wen Hsu[a)]
Laboratory of Atmospheric and Space Physics, University of Colorado Boulder, Colorado 80309

Mihály Horányi[b)]
Laboratory of Atmospheric and Space Physics, Colorado Center for Lunar Dust and Atmospheric Studies, NASA Lunar Science Institute, University of Colorado Boulder, Colorado 80309

(Received 28 September 2011; accepted 16 March 2012)

We have selected video images from the Apollo 16 mission and analyzed the motion of dust clouds kicked up by the wheels of the Lunar Roving Vehicle (LRV). Applying the equations of ballistic motion, we estimate both the velocity of the dust and the gravitational field strength at the lunar surface. From measurements of the rotation of an LRV wheel, we estimate the speed of the LRV. Such exercises can be useful when discussing ballistic trajectories and angular motion in a high school or introductory level college physics class. © *2012 American Association of Physics Teachers.*
[http://dx.doi.org/10.1119/1.3699957]

I. INTRODUCTION

In April 1972, during the Apollo 16 mission, the Lunar Roving Vehicle (LRV) was used to explore the Descartes crater.[1] The LRV was a battery-driven vehicle that provided the Apollo astronauts with greater mobility during their extra-vehicular activities (EVAs) on the lunar surface. The Apollo TV camera provided high resolution color video that was transmitted in real-time to Earth. Footage recorded during a high-speed traverse by LRV—the "Lunar Grand Prix"—showed copious amounts of dust kicked up by its wheels. The dust clouds were produced intermittently with different maximum heights and densities. Figure 1 shows the so-called "rooster tails" in two series of images from the Apollo 16 video footage.

These lunar dust trails resemble those produced by a vehicle with paddle tires on a terrestrial sandy surface. For a tenuous dust cloud, where the inter-particle collisions are rare, a dust particle follows a ballistic path from its ejection until it returns to the surface. The shape of the trajectory is determined by the gravitational acceleration and the initial velocity of the dust. The LRV dust trails provide an unusual opportunity for quantitative analysis of ballistic motion on a celestial body with gravity significantly lower than Earth's ($g_E = 9.8\ \mathrm{m/s^2}$; $g_M = 1.6\ \mathrm{m/s^2}$).

II. ANALYSIS OF "THE LUNAR GRAND PRIX" FOOTAGE

As is the case for most modern video cameras, the frame rate of the TV camera used during the Apollo 16 mission was 29.97 fps.[2] The footage was digitally scanned and transformed into a series of images. Each image corresponds to one video frame. For our analysis, we chose periods of time when the velocity vector of the LRV is approximately constant and orthogonal to the camera line of sight. This choice simplifies the analysis to a two-dimensional geometry. The front wheel of the LRV had a radius $R = 16$ in. (40.65 cm), and its rotation can be easily followed in the images. The resolution of the images is 720×480 pixels. Using the front wheel as a length scale, we found that 1 pixel in an image from our clips corresponds to a length of from 1.5 to 2 cm at the distance of the LRV from the camera. We chose a coordinate system with its origin fixed to the rear fender of the LRV. The X-axis extends horizontally to the right, and the Z-axis points upward perpendicular to the X-axis (see Fig. 2).

The dust particles move as projectiles, and their positions can be described by

$$x = X_0 + V_{X_0} t, \tag{1}$$

$$z = Z_0 + V_{Z_0} t - \frac{1}{2} g_M t^2, \tag{2}$$

where t is the elapsed time, g_M is the gravitational field strength on the surface of the Moon, and (X_0, Z_0) and (V_{X_0}, V_{Z_0}) are, respectively, the initial position and velocity of a dust cloud structure in our coordinate system. The time interval between frames is fixed by the frame rate to be 1/29.97 s. With values of X and Z measured as functions of time, Eqs. (1) and (2) can be used to estimate both the initial speed of the dust relative to the LRV and the gravitational field strength on the Moon's surface.

On each image, we measure the location of the rear fender and the position of the top of the dust cloud and then transform these measurements to our coordinate system. For example, $X_m = \left(X_{\mathrm{dust[pixel]}} - X_{\mathrm{fender[pixel]}}\right) \times \mathrm{scale}\,[\mathrm{m/pixel}]$ where X_m is the measurement to be used in Eqs. (1) and (2), and $X_{\mathrm{dust[pixel]}}$ and $X_{\mathrm{fender[pixel]}}$ are the coordinates measured on the image; "scale" is the scale-factor used to convert differences between pixels to lengths in meters.

In most images, the rear fender can be located precisely. On the contrary, the lofted dust cloud is a diffuse, time-varying structure, and it is difficult to track precisely any specific blob of dust through its entire excursion. To minimize this uncertainty, we measure the upper tip of the dust cloud. The dust at the top of a rooster tail has the largest V_{Z_0}. These dust particles do not intermix with grains coming off the surface with lower initial speeds. Thus, with no air resistance and no collisions with other particles, the motion of these lofted dust grains is affected only by lunar gravity. The location of the tip of the dust cloud can initially be identified precisely, but as the cloud reaches its maximum height, it becomes increasingly dispersed, and measurement errors increase.

The LRV ground speed (V_{LRV}) can be estimated from the rotation of the wheel by measuring the angular motion of the spoke. We measured the spoke of the front left wheel because it remains mostly unobscured by the lofted dust. The spoke can be identified as a high-contrast, elongated structure at the

 © 2012 American Association of Physics Teachers

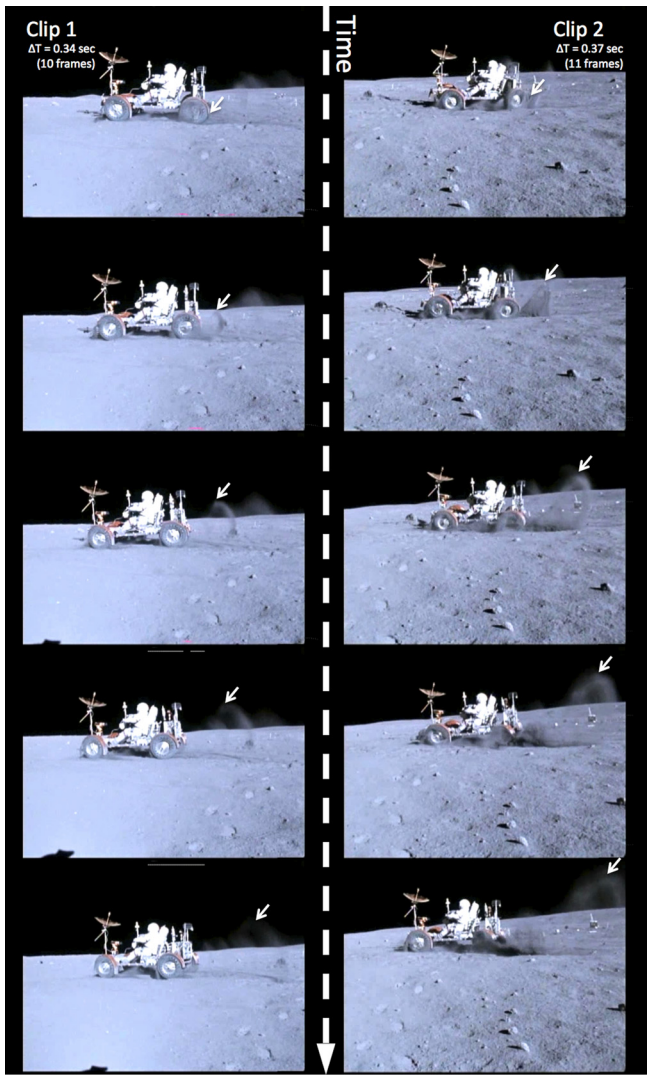


Fig. 1. (Color online) Two clips from the Apollo 16 "Grand Prix" footage used in this work. The time series of images from the clip 1 are in the left column; those from clip 2 are in the right column. Arrows indicate the subsequent positions of the dust cloud structure. The time interval between the images shown here is 0.34 s (10 frames) for clip 1 and 0.37 s (11 frames) for clip 2.

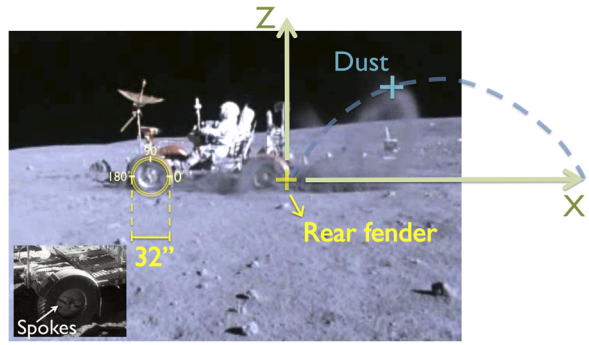


Fig. 2. (Color online) The coordinate system and the length-scale used in this work. The 2D coordinates system is centered and fixed at the rear fender. The location of the top of the dust cloud is marked by a cross. The front wheel and the rotation angle of its spoke are also shown. The spokes are shown in the lower-left inset image.

side of the wheel. The rotation angle θ is taken to be zero when the spoke points to the rear of the LRV, and to increase positively in the counter-clockwise direction (see Fig. 2). The rotation angle of one of the two spokes is recorded in each frame. We assume that the LRV moved with constant speed, and we fit the measurements of the rotation angle to

$$\theta = \theta_0 + \Omega t, \tag{3}$$

where θ_0 is the initial angular position of the spoke and Ω is the angular speed of the wheel. The LRV speed is then given by

$$V_{\mathrm{LRV}} = R\Omega. \tag{4}$$

III. RESULTS

Two clips from the footage were chosen for this work (see Fig. 1). There are 41 frames in clip 1 and 46 in clip 2. Figures 3 and 4 show the measured positions as functions of time. The uncertainty of the dust cloud location is estimated from the diffuseness of the cloud. The measured horizontal and vertical positions of the dust are fitted independently to Eqs. (1) and (2)

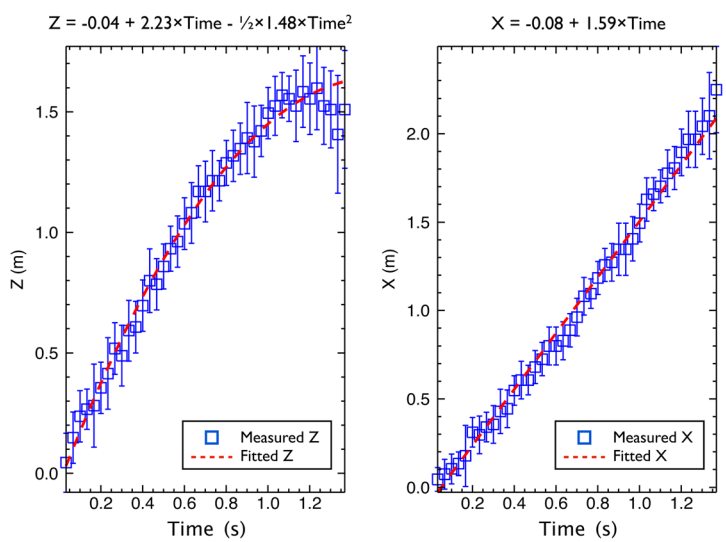


Fig. 3. The measured and fitted dust positions (left panel: Z; right panel: X) as a function of time for video clip 1. The measured data are shown (squares) with error bars. The dashed line fitting the data has the equation shown above the plot.

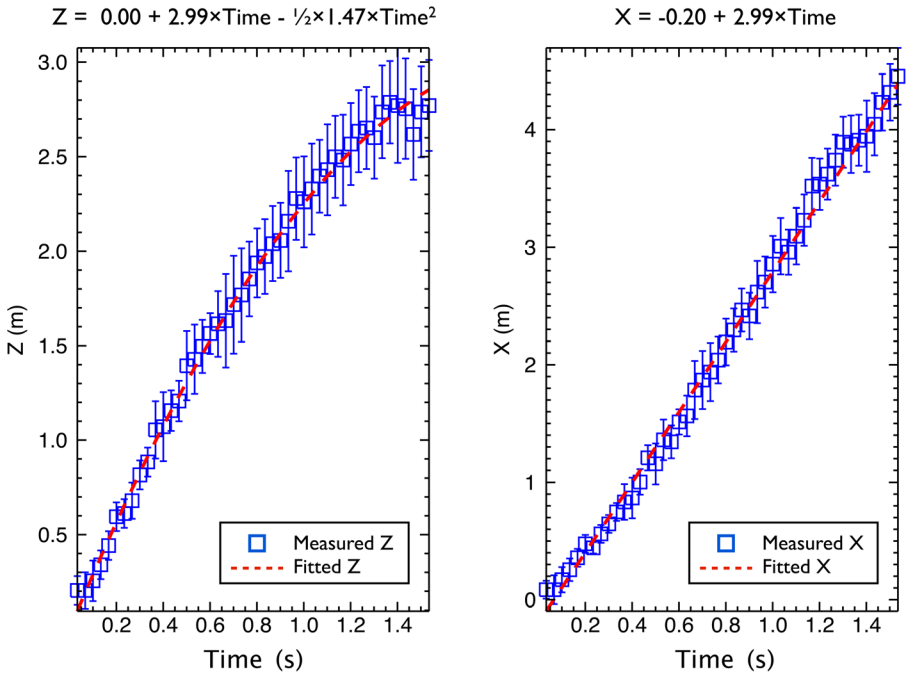


Fig. 4. The measured and fitted dust position for video clip 2. The symbols are as described in Fig. 3.

using a least squares minimization method.[3] The measured rotation angles of the spoke are shown in Figs. 5 and 6, and it is fitted to Eq. (3). The initial position (X_0, Z_0), initial velocity (V_{X_0}, V_{Z_0}), lunar gravitational field strength (g_M), and LRV speed (V_{LRV}) determined from these measurements are listed in Table I.

As expected, the initial positions of the dust cloud structures are almost coincident with the origin of our coordinate system. The value of g_M determined from these two clips is within 10% of the true value, a result well within our error estimates. The speeds $V_0 = (V_{X_0}^2 + V_{Z_0}^2)^{1/2}$ of the tip of the dust cloud relative to the LRV are 2.7 ± 0.1 m/s for clip 1 and 4.2 ± 0.1 m/s for clip 2. The LRV ground speed obtained from the rotation angle of the wheel is about 2.5 m/s (9 km/h or 5.6 mph). The actual speed is most likely slower as we did not consider wheel slippage in our analysis.[4] These numbers are certainly reasonable given that the reported average speed of the LRV during the Lunar Grand Prix is less than 10 km/h.[6] The initial velocity vector of the dust cloud has an angle of 55° and 45° to the horizontal direction, indicating a well-designed and functioning fender.

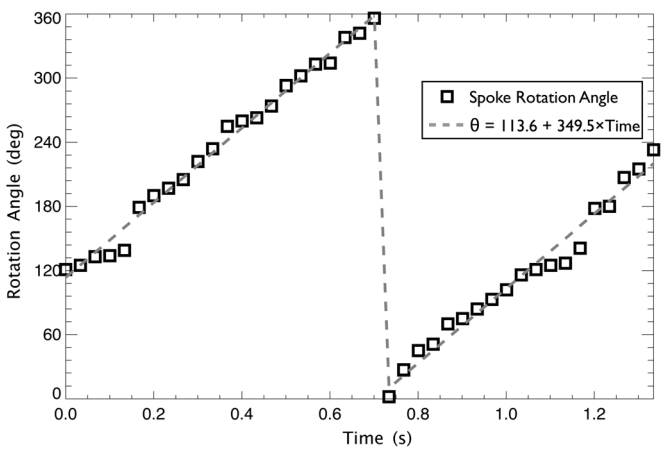


Fig. 5. The spoke rotation angles measured from video clip 1. The squares represent the measured rotation angle (θ) as a function of time and the gray dashed line shows the fit of Eq. (3). The estimated rotation rate is $\Omega = 349.5 \pm 3.6$ deg/s.

IV. DISCUSSION

On the lunar surface, dust thrown up by the LRV wheels is expected to follow a ballistic trajectory. The dust cloud as a whole, however, forms characteristic rooster tails, as opposed to simple parabolic arcs. The lofted dust particles have a wide distribution of initial velocities, and the superposition of their many different parabolic trajectories produces the rooster tails. The ballistic motion is revealed only when tracking grains with identical initial velocities, as we have done for the dust population with the largest V_{Z_0}.

In Fig. 7, we plot calculated trajectories along with our measurements of the positions of the dust in clip 1. Our measurements cover only the ascent part of the trajectory,

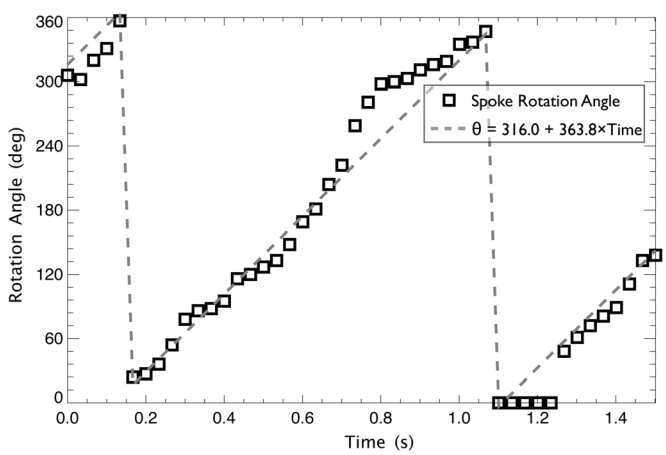


Fig. 6. The spoke rotation angles measured in video clip 2. The symbols are as described in Fig. 5.

Table I. Parameters that fit the ballistic motion equation [Eqs. (1) and (2)] to the data from the two clips.

	X_0 (m)	Z_0 (m)	V_{X_0} (m/s)	V_{Z_0} (m/s)	g_M (m/s^2)	V_{LRV} (m/s)
Clip 1	-0.08 ± 0.03	-0.04 ± 0.06	1.59 ± 0.04	2.23 ± 0.20	1.48 ± 0.29	2.5 ± 0.03
Clip 2	-0.20 ± 0.03	0.00 ± 0.05	2.99 ± 0.05	2.99 ± 0.19	1.47 ± 0.27	2.6 ± 0.05

and they generally lie between the trajectory calculated with our value of g_M (upper solid black curve) and the trajectory calculated using the true value (lower solid black curve).

The shape of a ballistic trajectory is determined by the initial dust velocity, the gravitational field strength, and the air drag (if an atmosphere is present). The first two of these factors are mathematically coupled in this type of analysis. Let $V_{Z_0} = V_0 \sin\delta$, where δ is the angle between V_0 and the ground. Then, for $X_0 = Z_0 = 0$, Eq. (2) becomes

$$z(x) = (\tan\delta)x - \frac{g_M}{2V_0^2\cos^2\delta}x^2. \tag{5}$$

Equation (5) describes the parabolic shape of a ballistic trajectory in vacuum. Because X, Z, and δ are measurable quantities, the video images actually provide V_0^2/g_M from which we can extract g_M after we have used the appropriate spatial and temporal scale factors to obtain V_0.

It is interesting to note that on Earth where $g_E = 9.8$ m/s^2, an initial velocity of the dust particles $V_0^E = V_0^M(g_E/g_M)^{1/2}$ would result in a trajectory identical to one on the Moon if there were no atmospheric drag. For (very) small particles of mass m moving with speed v in air at standard temperature and pressure (STP), the drag force is well approximated as $F = -\beta v d$, where d is the diameter of the particle and $\beta = 1.6 \times 10^{-4}$ N s m^2 (cf. Ref. 5). When such (linear) drag is included, Eqs. (1) and (2) become[5]

$$x(t) = X_0 + V_{X_0}\tau\left(1 - e^{-t/\tau}\right), \tag{6}$$

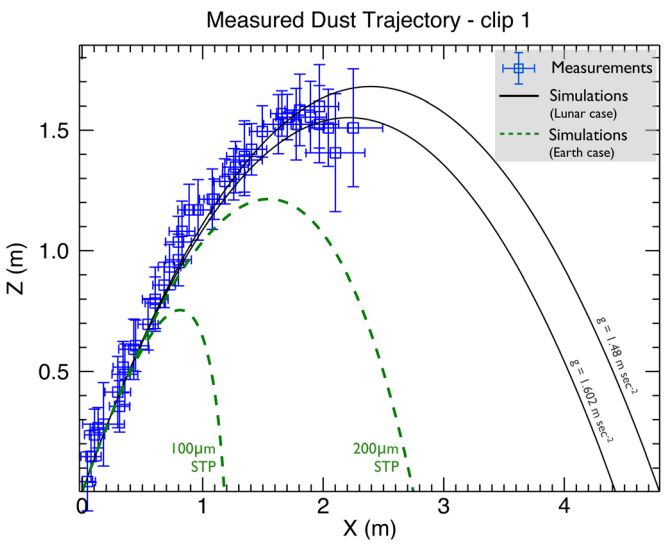


Fig. 7. Comparison of the measured dust trajectory (clip 1) and calculated trajectories. Squares represent measurements. The upper solid curve is the trajectory calculated using our value of g_M; the lower solid curve is the trajectory calculated using the true lunar gravitational field strength. For comparison, the dashed curves show the trajectories of 100 μm and 200 μm radius dust particles on Earth with the effects of air drag taken into account via Eq. (8).

$$z(t) = Z_0 + (V_{Z_0} + V_t)\tau\left(1 - e^{-t/\tau}\right) - V_t t, \tag{7}$$

where $\tau = m/(\beta d)$ is the time it takes the horizontal speed to reach $1/e$ of its initial value, and $V_t = g\tau$ is the terminal speed of a particle. Thus, the effect of (linear) drag is to alter Eq. (5) for the trajectory to

$$z = \left(\frac{V_{Z_0} + V_t}{V_{X_0}}\right)x + V_t\tau\ln\left(1 - \frac{x}{\tau V_{X_0}}\right). \tag{8}$$

By expanding the natural log to second order you can show that this equation reduces to Eq. (5) in the limit of no drag (as $\tau \to \infty$).

Because of the drag force, the shapes of ballistic trajectories on Earth are strongly dependent on the size of the dust particles. Figure 7 shows the trajectories on Earth for two different particle sizes using Eq. (8). As Fig. 7 shows, air drag causes the dust trajectories to become asymmetric with respect to their apexes. The fact that our measurements show no deceleration in the X-direction (see the right panel of Figs. 3 and 4) confirms that the footage was recorded in an airless environment.

The images and the measurements described above are available as supplementary material[6] and can also be found at the Colorado Center for Lunar Dust and Atmosphere Studies (CCLDAS) website.[7] These materials can be used for high-school or freshman-level physics activities on ballistic and angular motion. The video footage also has with it the astronauts' dialogue transcript,[8] which adds a nice human component to a scientific discussion. Combined with the historical background of the Apollo mission, this 40-year-old footage could be useful for broad interdisciplinary team-teaching projects that combine topics in Earth and planetary science, technology development, and the future of human space exploration.

V. SUMMARY

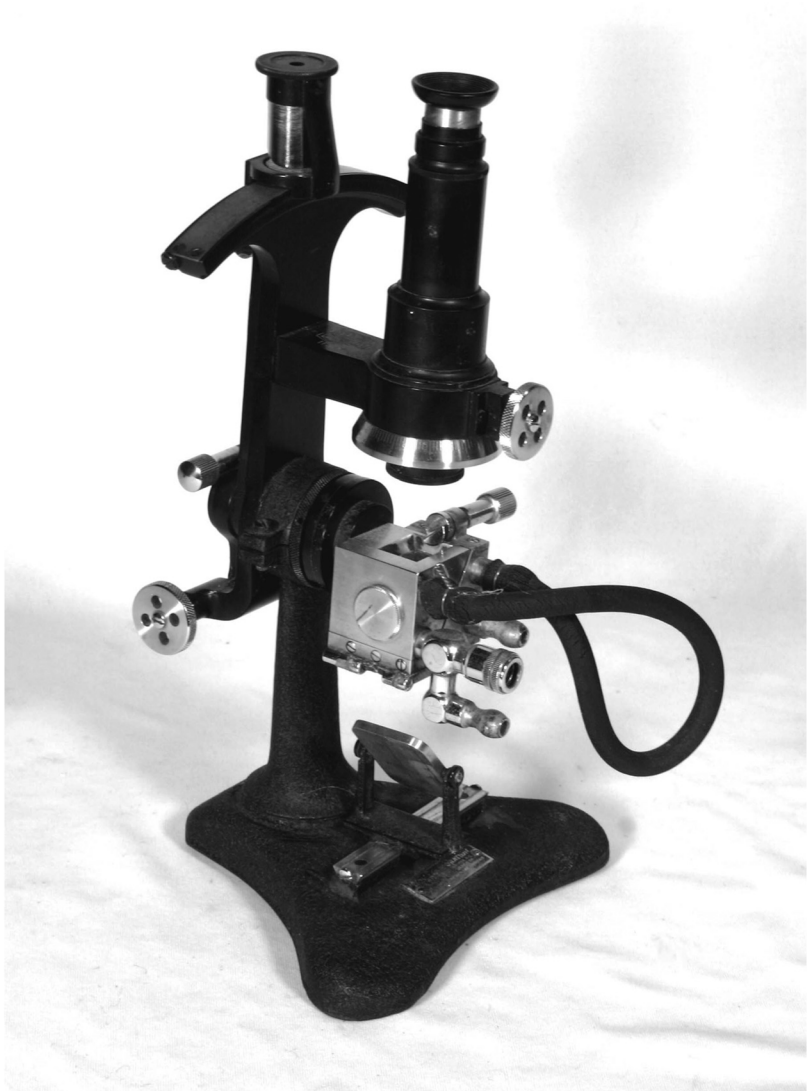
We have analyzed the motion of the dust clouds lofted by the Lunar Roving Vehicle of the Apollo 16 mission. Adopting a simple 2D geometry, we found that the dust followed ballistic trajectories under the influence of the lunar gravity. The gravitational constant of the moon derived from the dust trajectory is within 10% of the expected value. The images used in our analysis are available online for use as supplementary material in physics education.

ACKNOWLEDGMENTS

This work was supported by the NASA Lunar Institute's Colorado Center for Lunar Dust and Atmospheric Studies. The authors thank Hemal Semwal for his participation in this work. The authors thank Marcus Piquette for uploading the online material to the CCLDAS website. The authors acknowledge the helpful comments by the anonymous referees.

[a]Electronic mail: sean.hsu@lasp.colorado.edu
[b]Electronic mail: mihaly.horanyi@lasp.colorado.edu

[1]"Apollo 16 Preliminary Science Report," NASA Manned Spacecraft Center, 1972, available online at <http://www.hq.nasa.gov/alsj/a16/as16psr.pdf>.
[2]"Apollo color television subsystem: Operation and training manual," Westinghouse Defense and Space Center, 1971; document courtesy of Stan Lebar.
[3]W. H. Press, S. A. Teukolsky, W. T. Vetterling, and B. P. Flannery, *Numerical Recipes in C: The Art of Scientific Computing*, 2nd ed. (Cambridge U.P., Cambridge, MA, 1992).
[4]C. Howell Mullis, "A Study and Analysis of the MSFC Lunar Roving Vehicle Dust Profile Test Program," Bureau of Engineering Research Report 139-92, College of Engineering, University of Alabama, 1971, available online at <http://www.hq.nasa.gov/alsj/19720007590_1972007590.pdf>. PDF document courtesy of NASA Technical Reports Server. Experiments suggest that the slip might be more than 20%.
[5]J. R. Taylor, *Classical Mechanics* (University Science Books, South Orange, NJ, 2005).
[6]See supplementary material at http://dx.doi.org/10.1119/1.3699957 for information on Ballistic motion of dust particles in the Lunar Roving Vehicle dust trails.
[7]The CCLDAS website can be found at <http://lasp.colorado.edu/ccldas/RoosterTail.html>.
[8]*Apollo Lunar Surface Journal*, edited by E. M. Jones and K. Glover (Apollo 16—The First EVA—Grand Prix, available online at <http://www.hq.nasa.gov/alsj/a16/a16.trvlm1.html>).



Abbe Refractometer. Chemists often use physical techniques to characterize and identify materials. In particular, they use the Abbe refractometer to measure indices of refraction of solids and liquids. The device was invented by Ernst Abbe (1840-1905) in 1869 while working for the Zeiss Company in Jena. In addition to measuring the index of refraction to ± 0.0001, it can also be used to measure the dispersion of the material using the Fraunhofer C and F lines (656 and 486 nm). This instrument was made by the Spencer Lens Company and was sold in the 1940 era by Cenco for $265. It is in the Greenslade Collection. (Notes and photograph by Thomas B. Greenslade, Jr., Kenyon College)

View publication stats